

An Investigation of Statistical Power of [^{15}O]- H_2O PET Perfusion Imaging: The Influence of Delay and Time Interval

Rudie Kortekaas and Janniko R. Georgiadis

Contents

6.1	Introduction.....	140
6.1.1	Using PET to Study Brain Function	140
6.1.2	Optimization of PET Studies of the Brain	141
6.2	Materials and Methods.....	142
6.2.1	Participants and Imaging Procedures.....	142
6.2.2	Experimental Tasks	142
6.2.3	Data Preprocessing	143
6.2.4	Statistical Analysis.....	143
6.3	Results.....	143
6.3.1	SPM Analysis.....	143
6.3.2	TAC Analysis	146
6.4	Discussion.....	146
	Conclusion	147
	References.....	148

Abstract

In the study of human brain functions, positron emission tomography (PET) makes significant contributions in the form of “activation studies.” Activation studies with [^{15}O]- H_2O exploit the phenomenon that activated brain regions have altered perfusion by blood. Statistical comparing of two conditions or groups on a voxel basis yields an activation map. Because blood delivery to the brain is spatially and temporally inhomogeneous, we hypothesized a strong dependency

R. Kortekaas, PhD (✉)

Department of Neuroscience, Neuroimaging Center, University Medical Center Groningen, University of Groningen, 196, Groningen 9700 AD, The Netherlands

e-mail: r.kortekaas@umcg.nl

J.R. Georgiadis, PhD

Section Anatomy, Department of Neuroscience, University Medical Center Groningen, University of Groningen, 196, Groningen 9700 AD, The Netherlands

e-mail: j.r.georgiadis@umcg.nl

of the activation map on the time periods that are compared. We aimed to systematically chart this influence in order to optimize sensitivity and time resolution.

Methods: We dynamically scanned 11 volunteers with [^{15}O]- H_2O while they performed a motor task and a control task. We localized statistical differences between the tasks with a statistical parametric mapping on all possible permutations of consecutive frame summations.

Results: There was robust activation in the cerebellum and sensorimotor cortex and results were statistically most significant for the period 20–50 s. Intervals as short as 10 s also yielded statistically significant brain activations. The size of the activated clusters was strongly dependent on the interval that was compared and the optimal interval was different for the two locations.

Conclusion: Cluster size was indeed strongly influenced by time interval and location in interaction, but cluster significance appeared independent of location. Time periods of 10 s (20–30 or 30–40 s) were feasible, but maximal statistical power was obtained for 20–50 s durations. This knowledge allows maximization of sensitivity of [^{15}O]- H_2O PET experiments through rational experimental and statistical design.

Abbreviations

ANOVA	Analysis of variance
ASL	Arterial spin labeling
CBF	Cerebral blood flow
fMRI	Functional MRI
MRI	Magnetic resonance imaging
PET	Positron emission tomography
rCBF	Regional CBF
SPM	Statistical parametric mapping
SPSS	Statistical package for the social sciences
TAC	Time-activity curve

6.1 Introduction

6.1.1 Using PET to Study Brain Function

Many different techniques and scientific disciplines have played a role in building up our current understanding of the brain. PET has been a great contributor because it can be used to study a myriad of cerebral processes, structures, and molecules. PET has a very strong and ongoing role in imaging of receptors, enzymes, and nucleic acids.

Another important contribution that PET continues to make to brain science is the real-time identification of activated brain areas. Brain activation studies exploit the temporary increase in metabolism that occurs when a brain area is activated.

This increase in metabolism induces extra blood flow to that area and a larger glucose extraction from that blood. PET can detect both the extra blood flow and the enhanced glucose capture.

Brain activation studies with [¹⁵O]-H₂O PET exploit the phenomenon that regional cerebral blood flow (rCBF) in activated brain regions is increased. This increase changes the kinetics of injected [¹⁵O]-H₂O. To detect blood flow in the brain, the scientist, doctor, or medical nuclear worker injects a bolus of [¹⁵O]-H₂O into a large vein, usually in the arm. This bolus travels to the heart via the vena cava and then to the lungs via the pulmonary artery, mixing with blood as time progresses. During the passage through the lungs the [¹⁵O]-H₂O in the blood is joined by fresh oxygen (O₂) and travels along the pressure gradient back to the heart via the pulmonary vein. One-fifth of the blood with its dissolved [¹⁵O]-H₂O and oxygen then travels to the brain via the carotid arterial system and the vertebral arterial system, both of which connect to the circle of Willis. All arteries that penetrate into the brain tissue itself arise from the vertebral arterial system and the circle of Willis. These arteries carry [¹⁵O]-H₂O and oxygen to all brain areas but to an even larger extent to brain areas that are more active.

A series of brain scans are made with the PET camera, usually under different conditions. Activation maps, familiar as pictures of the brain with superimposed “activations,” can then be generated by statistically comparing the summed activity over a specific time interval between a task and a control task. The final result, including the statistical power and hence the size of the “activations,” depends on a number of choices that have to be made by the researcher.

6.1.2 Optimization of PET Studies of the Brain

One of the most important choices to make in PET data analysis is the time intervals to compare. We will thoroughly describe what the effect of the time interval is on the activations that are induced by different tasks.

The time interval is defined by the researcher by choosing the value of two parameters: the duration of the interval and its onset relative to tracer arrival in the brain. The duration of the time interval determines the temporal resolution of the measurement. Most [¹⁵O]-H₂O PET studies compared time periods of 1.5–2 min. The reason for this is that this results in relatively high statistical power (Kanno et al. 1991; Silbersweig et al. 1993) through the collection of a relatively large amount of disintegrations. However, this does not imply that PET methodology is unable to detect brain activation in shorter time intervals (Cherry et al. 1995; Gold et al. 1997; Hurtig et al. 1994; Silbersweig et al. 1995, 1993, 1994; Volkow et al. 1991). Not surprisingly, for short tasks or short stimuli, it is best to compare short intervals, provided that the stimulus occurs during the tracer uptake phase (Silbersweig et al. 1993; Volkow et al. 1991).

This indicates that not only the length of the time interval determines the result but also the timing of the interval relative to tracer arrival in the brain. So far, there does not appear to be a real consensus about the optimal start and length of the interval to take into consideration.

This could be due to differences between studies in data analysis (SPM or other methods), on stimulus or task duration, but also on the type of task. The type of task determines the brain areas activated, and because the delivery of blood to the brain is inhomogeneous in time and space (Ito et al. 2003, 2000), the optimal start and duration of the compared time period may differ between regions.

As far as we could determine, no systematic descriptions of the dependency of activation maps on start and duration of compared time interval have yet been published for [^{15}O]- H_2O PET. Also, no regional differences in these dependencies have been described yet.

Here we aimed to characterize the dependence of the activation map (both size and significance of activated clusters) on the following: (1) The duration of the compared interval. Is it always better to compare long intervals for ongoing tasks? (2) The onset of the compared interval. Should one compare early intervals or late intervals? From this we aimed to investigate regional differences in the optimal time period with the ultimate aim to predict optimal time intervals for a given brain region. To arrive at optimized regional sensitivity of [^{15}O]- H_2O PET through rational experimental and statistical design, we used a PET dataset with two homogeneous experimental tasks and analyzed all possible permutations of consecutive frame summations for statistical differences.

6.2 Materials and Methods

6.2.1 Participants and Imaging Procedures

Detailed methods have been published elsewhere (Georgiadis et al. 2006), but, briefly, 11 healthy right-handed females (mean age 34, range 21–47) participated after written informed consent according to the Declaration of Helsinki. Experimental procedures were approved by the Medical Ethics Committee of the University Medical Center Groningen. Five hundred MBq of [^{15}O]- H_2O was injected at 8 ml/s into the right antecubital vein. Eight 2-min scans were made with 8 min in between. Scans consisted of six 10-s frames and one 1-min frame. Scans 2–8 had an extra 30-s frame at the start to measure background activity. Injection was at the start of the first 10-s frame.

6.2.2 Experimental Tasks

These scans were made in the context of our Sexual Health Research Program. The *control task* (scans 4 and 5) was passive reception of clitoral stimulation from their male partner. The *motor task* (scans 2 and 3) consisted of the same stimulation, but additional rhythmic contraction of the muscles of hip, buttock, abdomen, and pelvic floor. The other scans were not used here. We selected these tasks for analysis because they (1) are homogeneous, (2) last over the entire scan, and (3) induce robust activations (Blok et al. 1997; Georgiadis et al. 2006; Seseke et al. 2006). Tasks that were not analyzed for this report were the first scan (passive rest) and the

last three scans (attempted orgasm). Brain activation due to stimulation and orgasm have been published elsewhere (Georgiadis et al. 2006, 2009).

6.2.3 Data Preprocessing

After background correction, all resulting scans had seven frames. Spatial processing and statistical analysis were done with SPM (<http://www.fil.ion.ucl.ac.uk/spm/>). The frames within each scan were realigned, and the first 10-s frame was discarded from analysis because of low counts and relatively high variability. The remaining six frames were then summed in all possible permutations of consecutive frames (see also Fig. 6.1). The summed images were spatially normalized (affine only) to the SPM [¹⁵O]-H₂O template and smoothed with a 10-mm kernel.

6.2.4 Statistical Analysis

Data from all experimental tasks were modeled with a general linear model, with a proportional scaling step. Volunteers and experimental tasks were modeled as factors (multi-subject: conditions and covariates). Contrast images between *motor task* and *control task* were calculated for all the different time intervals. Statistical threshold was set to $p < .001$, uncorrected for multiple comparisons. Glass brains with activated voxels as a function of the selected time interval are presented in Fig. 6.1. The size of reported and displayed clusters is at least eight voxels.

We used the number of activated voxels in the activated clusters and its Z value as a primary outcome (Fig. 6.2).

Finally, we constructed time-activity curves (TACs) for the activated clusters in order to verify and illustrate the results from SPM comparison of the different intervals (Fig. 6.3). With the program Amide (<http://amide.sourceforge.net/>), TACs were constructed as follows. First, ellipsoid ROIs were drawn over the activated foci in the sensorimotor area (22.6 mL) and the cerebellum (19.0 mL) on a subject by subject basis. To correct for injected radioactivity dose per scan, we used an ellipsoid covering the whole brain (3.11 L), calculated the mean radioactivity concentration over the final five frames, and divided all time points in the sensorimotor and cerebellar ROI by this value.

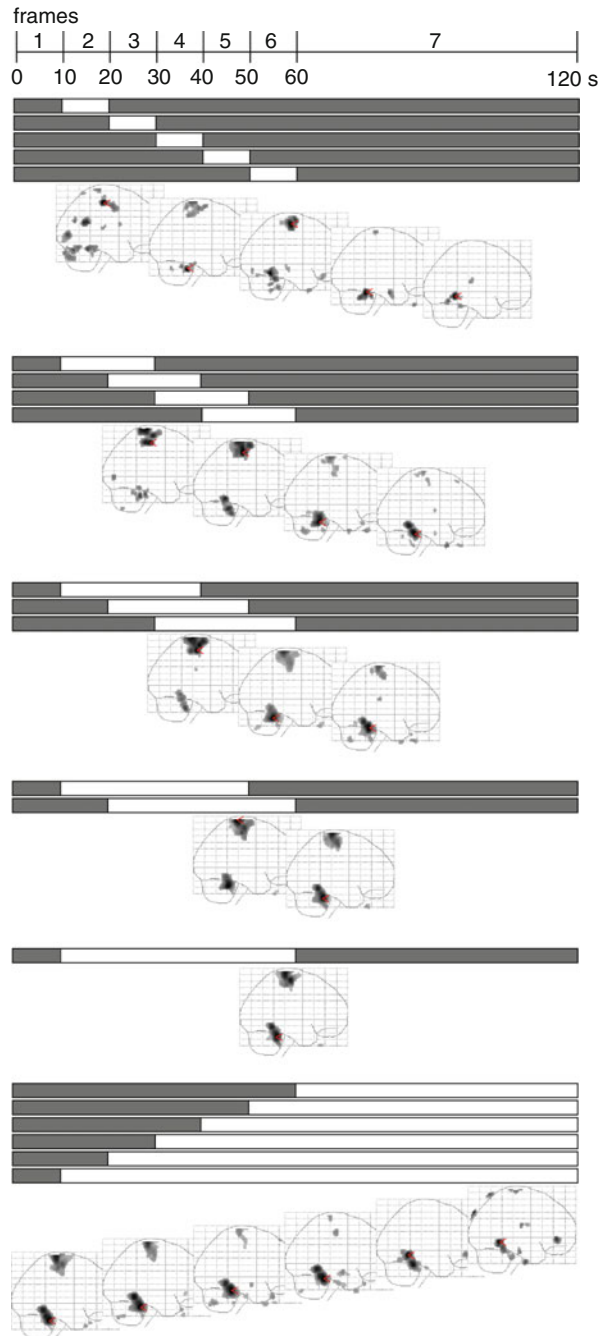
We performed ANOVA repeated measures (SPSS 12.0.2, Chicago, IL, USA) on the TACs with region, task, and time as factors.

6.3 Results

6.3.1 SPM Analysis

Figure 6.1 shows the intervals that were compared (in white) along with the brain activation patterns (t -distribution maps in a lateral glass brain) that resulted from all of these comparisons.

Fig. 6.1 The same contrast analysis, *motor task* versus *control task*, resulted in markedly different activation patterns depending on the time interval that was analyzed (indicated by *white bars*). *Small arrows* in the glass brains indicate the voxel with the highest *t*-value. All results are thresholded at $p_{\text{uncorrected}} < 0.001$



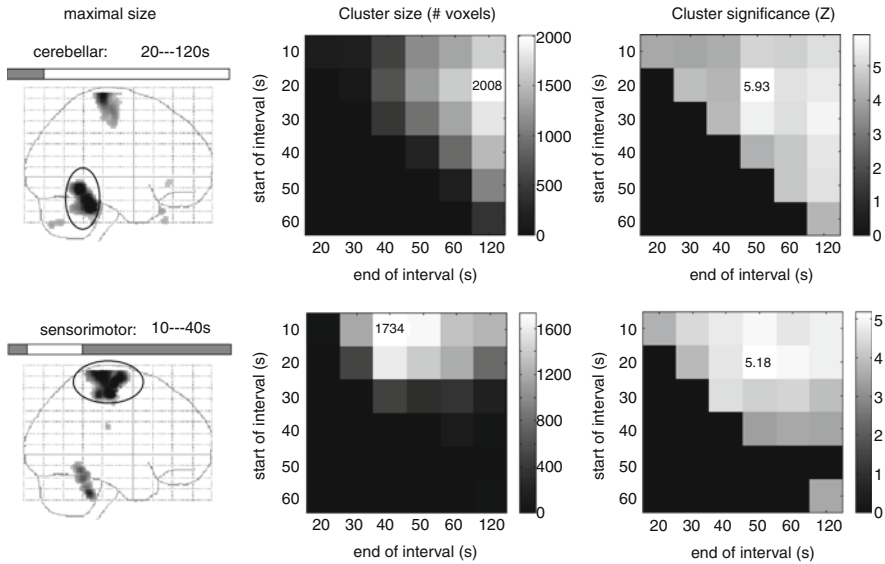


Fig. 6.2 The same contrast analysis, *motor task* versus *control task*, resulted in different results, depending on the time interval that was analyzed. Two clusters (*first column*) had different sizes (*middle column*) and different statistical significance (*last column*) depending on the period. The largest activation in sensorimotor cortex was found for the period 10–40 s while for cerebellar it was obtained for 20–120 s. The statistical power for both clusters was maximal for the period 20–50 s

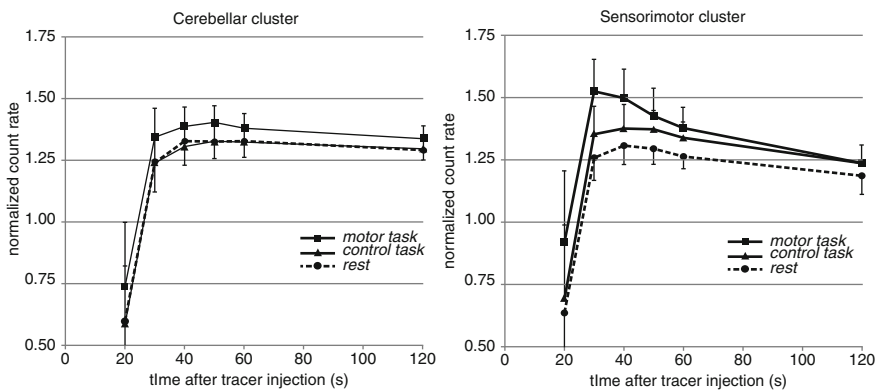


Fig. 6.3 Average time-activity curves (TACs) for the two activated clusters in relation to the tasks: in the *motor* condition the sensorimotor cluster is more dynamic and reaches a higher radioactivity concentration. Count rates were normalized intrascan to the average whole-brain activity concentration in the last five frames. *Error bars* indicate standard deviations over subjects

Two robust brain activation loci were present for in the majority of compared intervals: the dorsal sensorimotor cortex and the medial part of the anterior cerebellum. As can be seen in the top rows of this figure, significant rCBF differences were also found with the shortest duration of the time period: 10 s. The 10 s interval that

resulted in the largest activation was 30–40 s after injection of the radiotracer. The period compared clearly had a strong influence on the activation maps: both activation clusters were highly variable and the sensorimotor cluster was sometimes completely absent (for periods 50–60 and 50–120 s).

The sizes of the two clusters were very dependent on the time interval compared, and, moreover, the period resulting in maximum cluster size was very different for the two clusters. Figure 6.2 gives a matrix representation of the interval dependency of cluster size (middle column) and cluster significance (far right column).

For the cerebellar cluster, the maximum size was 2,008 voxels, which was reached by comparing 20–120 s after tracer injection between the two conditions (*motor* and *control*). However, the cerebellar cluster reached its highest significance ($Z=5.93$) for the period 20–50 s (top right in Fig. 6.2).

For the sensorimotor cluster, the maximum size was 1,734 voxels, but this was reached for a completely different interval: 10–40 s rather than 20–120 s. Not only is the optimum period much earlier, it is also much shorter for the sensorimotor cluster.

The highest significance ($Z=5.18$) for this cluster is, now identical to that for the cerebellum, found for the period 20–50 s (bottom right in Fig. 6.2).

6.3.2 TAC Analysis

TACs for the two regions are presented in Fig. 6.3. Visual inspection shows clear differences between the two anatomical areas. ANOVA repeated measures of the TACs confirmed this impression, revealing in addition to a strong time effect [$F(5)=49.63$, $p=0.02$] a strong interaction of time and region [$F(5)=30.49$, $p=0.032$]. (Interactions time \times task and time \times task \times region could not be investigated due to lack of residual degrees of freedom.)

The sensorimotor cluster reached higher radioactivity concentration in the *motor* condition than the cerebellar cluster, which was also more stable in time.

6.4 Discussion

In [^{15}O]- H_2O PET it is common to use SPM subtraction analysis on 1.5- or 2-min intervals, but it is unclear whether these intervals result in maximal cluster size or significance. Here, we aimed to systematically investigate the influence of time interval on these properties of activated clusters. We compared all possible permutations of consecutive frames of a *motor task* and a *control task*.

Overall, the main activated clusters in our tasks were in the anterior part of the cerebellum, including the anterior lobe of the vermis and deep cerebellar nuclei, and in the region of the dorsal precentral gyrus and paracentral lobule. Both these regions were also found in previous studies of voluntary pelvic muscle contractions (Blok et al. 1997; Georgiadis et al. 2006, 2009; Seseke et al. 2006). In all likelihood they represent the sensorimotor area of striated pelvic muscles and the functionally connected cerebellar domains.

The choice of the analyzed time interval had a profound influence on the overall activation map. In particular, the analysis gave maximal cluster size in the sensorimotor area when the interval 10–40 s was used, whereas for the cerebellum this was for the interval 20–120 s. So both the optimal onset and the optimal duration of the time period were regionally dependent.

The basis for this finding is the different temporal dynamics of the activity concentration in the two regions or, more precisely, the different dynamics of the difference between the curves for the two tasks between the two regions. The difference between the TACs for the two tasks was more or less constant for the cerebellum (Fig. 6.3, left pane), but for the sensorimotor area, the difference between the two curves was clearly larger during the first half of the scan (Fig. 6.3, right pane). This is in agreement with the SPM findings that comparing long intervals works best for the cerebellum and that, by contrast, comparing shorter earlier intervals works best for the sensorimotor area.

It is known that blood flow in the cerebellum is very different from that in the cerebral cortex. In particular, cerebellar CBF (Bauer et al. 1999; Ito et al. 2003; Tomita et al. 1978) and perfusion pressure (Ito et al. 2003, 2000) are among the highest in the brain. Because vascular water is extracted into brain tissue, but clearance from tissue is slow (Wong 2000), the rising phases of the TACs for the cerebellum and sensorimotor area are similar. It is not understood why the higher perfusion pressure in the cerebellar vasculature appears to reduce extraction of labeled water (more horizontal TACs than in the sensorimotor area) rather than to increase it.

In addition to the size of the activated cluster, the significance of the clusters was also highly dependent on the time interval compared. In this case, however, the time period yielding maximal values was the same for the cerebellar and sensorimotor cluster: 20–50 s.

Our results demonstrate that the analysis of continuously performed tasks is not necessarily most sensitive when long intervals are compared. Also, and this may not be the case for short events (Silbersweig et al. 1993; Volkow et al. 1991), including the washout phase into the analysis does not necessarily lead to smaller activations, although it does reduce significance. A surprising finding was that significant activations can readily be detected by SPM with intervals as short as 10 s, which is three times shorter than previously stated (Silbersweig et al. 1993).

[¹⁵O]-H₂O PET is a very sensitive technique albeit relatively old technique. By carefully choosing the time interval of interest, guided by the region of interest, it is possible to achieve dramatic increases in sensitivity compared to the commonplace method of comparing 1.5- or 2-min intervals. Cerebellar activation is best studied with longer intervals while sensorimotor area activations can be best detected with shorter, early intervals, even if the task is carried out for much longer.

Conclusion

In conclusion, we were able to derive which time intervals gave maximally sized activations and maximal significance in two distinct brain areas. This knowledge allows maximization of sensitivity of [¹⁵O]-H₂O PET activation studies through rational experimental and statistical design.

References

- Bauer R, Bergmann R, Walter B et al (1999) Regional distribution of cerebral blood volume and cerebral blood flow in newborn piglets—effect of hypoxia/hypercapnia. *Brain Res Dev Brain Res* 112:89–98
- Blok B, Sturms L, Holstege G (1997) A pet study on cortical and subcortical control of pelvic floor musculature in women. *J Comp Neurol* 389:535–544
- Cherry SR, Woods RP, Doshi NK et al (1995) Improved signal-to-noise in pet activation studies using switched paradigms. *J Nucl Med* 36:307–314
- Georgiadis J, Kortekaas R, Kuipers R et al (2006) Regional cerebral blood flow changes associated with clitorally induced orgasm in healthy women. *Eur J Neurosci* 24:3305–3316
- Georgiadis JR, Reinders AATS, Paans AMJ et al (2009) Men versus women on sexual brain function: prominent differences during tactile genital stimulation, but not during orgasm. *Hum Brain Mapp* 30:3089–3101
- Gold S, Arndt S, Johnson D et al (1997) Factors that influence effect size in 15o pet studies: a meta-analytic review. *Neuroimage* 5:280–291
- Hurtig RR, Hichwa RD, O’Leary DS et al (1994) Effects of timing and duration of cognitive activation in [15o] water pet studies. *J Cereb Blood Flow Metab* 14:423–430
- Ito H, Yokoyama I, Iida H et al (2000) Regional differences in cerebral vascular response to paco2 changes in humans measured by positron emission tomography. *J Cereb Blood Flow Metab* 20:1264–1270
- Ito H, Kanno I, Takahashi K et al (2003) Regional distribution of human cerebral vascular mean transit time measured by positron emission tomography. *Neuroimage* 19:1163–1169
- Kanno I, Iida H, Miura S et al (1991) Optimal scan time of oxygen-15-labeled water injection method for measurement of cerebral blood flow. *J Nucl Med* 32:1931–1934
- Seske S, Baudewig J, Kallenberg K et al (2006) Voluntary pelvic floor muscle control—an fmri study. *Neuroimage* 31:1399–1407
- Silbersweig DA, Stern E, Frith CD et al (1993) Detection of thirty-second cognitive activations in single subjects with positron emission tomography: a new low-dose H₂¹⁵O regional cerebral blood flow three-dimensional imaging technique. *J Cereb Blood Flow Metab* 13:617–629
- Silbersweig DA, Stern E, Schnorr L et al (1994) Imaging transient, randomly occurring neuropsychological events in single subjects with positron emission tomography: an event-related count rate correlational analysis. *J Cereb Blood Flow Metab* 14:771–782
- Silbersweig DA, Stern E, Frith C et al (1995) A functional neuroanatomy of hallucinations in schizophrenia. *Nature* 378:176–179
- Tomita M, Gotoh F, Sato T et al (1978) Comparative responses of the carotid and vertebral arterial systems of rhesus monkeys to betahistone. *Stroke* 9:382–387
- Volkow ND, Mullani N, Gould LK et al (1991) Sensitivity of measurements of regional brain activation with oxygen-15-water and pet to time of stimulation and period of image reconstruction. *J Nucl Med* 32:58–61
- Wong EC (2000) Potential and pitfalls of arterial spin labeling based perfusion imaging techniques for mri. In: Moonen CWT, Bandettini PA (eds) *Functional MRI*. Springer, Berlin/ New York